Proceedings of the 9ICEG
9th International Congress on Environmental Geotechnics
25-28 June, 2023 | Chania, Greece

https://doi.org/10.53243/ICEG2023-403

A novel sensor for in-situ thermo-mechanical testing and application to MICP-treated soils

Xiaoying Gu[1], Alexandra Clarà Saracho[2], Nikolas Makasis[3], Monika Johanna Kreitmair[4], Guillermo Narsilio[5], and Stuart Haigh[6]

[1]*The University of Melbourne, Victoria, Australia, email: annie.gu@unimelb.edu.au*

[2]*Assistant Professor, The University of Texas at Austin, Austin, United States, email: alexandra.clara.saracho@utexas.edu*

[3]*Reserach Associate, University of Cambridge, Cambridge, United Kingdom, email: nm735@cam.ac.uk*

[4]*Reserach Associate, University of Cambridge, Cambridge, United Kingdom, email: mk2040@cam.ac.uk*

[5]*Professor, The University of Melbourne, Victoria, Australia, email: narsilio@unimelb.edu.au*

[6]*Professor, University of Cambridge, Cambridge, United Kingdom, email: skh20@cam.ac.uk*

ABSTRACT

Microbially Induced Calcium Carbonate ($CaCO_3$) Precipitation (MICP) is an innovative technique for strengthening sandy soils that leads to the binding of soil grains with $CaCO_3$ crystals. These crystals can act as thermal bridges to enhance the soil's thermal conductivity, an important soil thermal property for assessing the efficiency of ground heat exchangers, which are used, for example, in energy geo-structures at shallow depths. The combination of energy geo-structure applications with MICP-treated soils is still in its nascency. While existing studies focus on thermal property changes, the quantification of changes in soil thermal conductivity under the in-situ stress state and during isotropic compression is overlooked due to limitation of current experimental techniques. Thermal conductivity measurements in this application require accurate, fast, and non-destructive sensors. However, conventional steady-state and transient thermal probe methods do not fulfill these criteria. The former suffers from long waiting times required to reach a steady state, making it unsuitable for measuring the thermal conductivity of unsaturated soils due to potential changes in the uniform water content of the sample. By contrast, measurement cycles of less than one minute can be achieved by transient thermal probes, but commercially available sensors are expensive, and can be destructive for some laboratory tests. This research introduces a novel transient sensor by miniaturising the traditional thermal probes into a “point” measurement with just a resistor and using a thermocouple to measure temperature change. The accuracy of the new sensor is investigated using numerical and experimental approaches. The developed sensor in this work provides an economical and non-destructive solution for in-situ and laboratory thermal sensing and can be used in other applications.

Keywords: MICP, thermal conductivity, sands, ground improvement, transient thermal probes; finite element model

1 INTRODUCTION

Increasing energy demand and the impacts of climate change highlight the need to turn to renewable sources of energy. One such source is geothermal energy, which can be harnessed for electricity generation (deep) as well as space heating and cooling purposes (shallow). Energy geo-structures (EGS) are an application of shallow geothermal energy, where construction costs are reduced by utilising subsurface infrastructure to exchange heat with the ground, instead of purpose-built structures. Current research has developed understanding on incorporating foundation piles (Bourne-Webb et al., 2016; Brandl, 2006), retaining walls (Barla et al., 2020; Makasis et al., 2020) and tunnel linings (Bidarmaghz et al., 2018; Insana et al., 2020) to serve as ground heat exchangers with little additional cost. Geothermal pavements is one of the energy geo-structure technologies that, while still in its nascency, is a cost-efficient, reliable, and sustainable solution for space heating and cooling throughout the world (Arulrajah et al., 2021; del-Castillo-García et al., 2013; Eugster, 2007; Gu et al., 2021).

Soil thermal conductivity has a significant impact on the amount of heat that is exchanged with the ground (Di Sipio et al., 2017; Kavanaugh, 2000) and it is thus a key parameter for designing and optimising the performance of geothermal systems. Notably, the heat storage capacity of soils decreases as a result of desaturation, with reported values of thermodynamic efficiency dropping by up to 40% in sand under dry conditions (Akrouch et al., 2015). This is why the applicability of EGS in areas where soils are partially-saturated due to poor rainfall or high evaporation can be limited (Venuleo et al., 2016).

Microbially induced calcium carbonate ($CaCO_3$) precipitation (MICP) has been widely applied within geotechnical engineering, targeting reduced erosion and liquefaction mitigation, amongst others (Clarà Saracho et al., 2021; DeJong et al., 2010; Mujah et al., 2016; P. Xiao et al., 2018). In addition, several MICP studies have highlighted the strength improvement and ground improvement cost reduction of road bases and sand materials (Porter et al., 2018; Rahman et al., 2020; Y. Xiao et al., 2022). Another application of MICP is enhancing the thermal conductivity of soils as it leads to the binding of soil particles by $CaCO_3$ crystals. This application can increase heat transfer rates in road bases which can be significant for geothermal pavement systems, increasing their performance and allowing for higher heating and cooling provision.

This work investigates MICP-treated sand for geothermal pavements, focusing on the sand thermal conductivity because heat transfer in soils occurs primarily by conduction (Haigh, 2012). Thermal conductivity can be affected by various factors, including soil structure, void ratio, and degree of saturation (Alrtimi et al., 2016; Chen, 2008), and MICP has the ability to bridge air or water-filled pores between soil particles, thus have a significant impact on the thermal conductivity (Narsilio et al., 2010; Yun et al., 2007). Research on the effect of MICP treatment on the thermal conductivity of soils is limited (Martinez et al., 2019; Venuleo et al., 2016; Y. Xiao et al., 2021). Venuleo et al. (2016) studied the influence of degree of saturation on thermal conductivity of MICP-treated sand, finding that the thermal conductivity of sand can be increased by up to 250%, with a greater increase at lower saturation levels. Y. Xiao et al. (2021) performed thermal conductivity tests on MICP-treated sands with different gradations, void ratios, and MICP treatment cycles, and established an empirical equation for predicting the thermal conductivity of MICP-treated silica sand. Since the principal function of pavements is transmitting loads to the subbase and underlying soil, the mechanical response of MICP-treated pavements may vary, in addition to the sand thermal conductivity. However, current research has focused on investigating the changes in thermal behaviour of MICP-treated sands, while studies to quantify the soil thermal conductivity under the in-situ stress state and during isotropic compression have been largely overlooked, perhaps due to experimental difficulties with current measurement techniques.

Extensive efforts have been made for the measurement of thermal conductivity in soils (Kersten, 1949). Measurement techniques can be broadly divided into two categories: steady state methods and transient methods (Alrtimi et al., 2016). Steady state methods use the principle of a longitudinal heat flow in steady conditions, while transient techniques measure the time-dependent energy dissipation process within a sample. The steady state guarded hot plate (GHP) method, and the transient thermal probe method are the most commonly used in industry for soil thermal conductivity measurement (Xamán et al., 2009). Yet, the GHP method suffers from long waiting times required to reach steady state, making it unsuitable for measuring the thermal conductivity of unsaturated soils due to potential changes in the uniform water content of the sample. By contrast, measurement cycles of less than one minute can be achieved by transient thermal probes, but commercially available sensors are scarce and relatively expensive instruments. Moreover, methods to quantify the thermal conductivity of soil under the in-situ stress state, as well as isotropic compression, have been largely overlooked. Most studies focus on the impact of porosity on the thermal conductivity of soil, and the majority of these methods involve compaction of several soil specimens at different water content levels and densities, leading to different soil structures which can affect thermal conductivity (Chen, 2008; Kersten, 1949). As a result, changes in the thermal conductivity between natural soils in-situ, and soils subject to field or laboratory load are largely unknown.

Here, we introduce a novel, cost-effective transient sensor to measure the thermal conductivity of soils. Transient thermal probes usually determine the thermal conductivity of a medium by comparing the rate of temperature change to that of an infinite line heat source within an infinite homogeneous medium. By replacing the line heat source with a resistance wire and using a thermocouple to measure the rate of temperature change, transient data can be acquired and used to determine the thermal conductivity of soils. However, given the assumptions associated with the infinite line heat source theory, the thermal

conductivities of the transient data are obtained using numerical modelling, simulating the heat transfer process in detail using finite element methods. The model is validated using untreated soil samples. To evaluate the accuracy of our new sensor, thermal conductivity values of MICP-treated sand specimens are measured using the GHP steady state method and compared to those measured using the transient sensor. This approach is adopted because the steady state method is considered more accurate and precise (Alrtimi et al., 2014; Nusier et al., 2003).

2 MATERIALS AND METHODS

2.1 Material and sample preparations

PVC cylindrical tubes of inner diameter and height of 42mm and 110mm, respectively, were dry packed with Hostun sand, a fine-grained, high-purity silica sand with characteristics given in Table 1. All specimens were prepared to the same target dry density by gently tapping their side with a tamping rod. The cores were oriented vertically using an acrylic bottom cap and a metallic filter mesh was placed adjacent to the bottom cap to prevent soil migration during the MICP treatment. Bottom ports were fitted with tubing to allow full control of drainage conditions during MICP treatment, as shown in Figure 1.

Sporosarcina pasteurii (strain designation DSM 33) was used for the MICP treatment of the soil specimens. Bacterial cultures were grown in DSMZ 220, containing 15g/L peptone from casein, 5.0 g/L peptone from soymeal, 5.0 g/L sodium chloride, and 20g/L urea. The bacteria solution was incubated at 30°C in a shaking incubator at 200 rpm to an optical density (OD_{600}) of 1.5. Before injecting 1 pore volume (PV, 60 ml) of the bacterial solution by gravity, 2 PV of deionized (DI) water were injected to ensure the specimen was fully saturated. Bacteria were allowed a 12-h retention period to attach to the sand particles before introducing 1 PV of the cementation solution, also from the top of the core. This procedure of injection-retention of the cementation solution was repeated every 24 h for each injection cycle until the desired number of injections was achieved. The cementation solution was a premixed solution of 3 g/L of nutrient broth in addition to urea and calcium chloride ($CaCl_2$) with a molar ratio of 1:1. All specimens were prepared in duplicates, with details of the injection scheme and the compositions summarised in Table 2. Following the MICP treatment, specimens were flushed with 2 PV of DI water to remove unreacted chemicals and dried for 24 h. The vertical profile of the $CaCO_3$ crystals precipitated inside the MICP-treated specimens was determined using inductively-coupled plasma optical emission spectrometry (ICP-OES), set to detect calcium. Details of the ICP-OES method can be found in Clarà Saracho et al. (2021).

Table 1. *Untreated sample characteristics (Rizvi et al., 2019; Seong et al., 2022)*

Untreated sand properties	**Houston sand**
Specific gravity, Gs	2.64
D_{50}:mm	0.33
C_u	1.7
Maximum void ratio, e_{max}	1.01
Minimum void ratio, e_{min}	0.555
Dry bulk density, ρ_d: g/cm^3	1.58
Porosity, n	0.40
Height: mm	110
Diameter: mm	42

Table 2. *Cementation treatment formulations*

Specimen name*:	Urea: M	Calcium chloride ($CaCl_2$): M	Nutrient broth: g/L	Number of injections	Injection point	Reaction time: h
S1-1, S1-2	0.3	0.3	3	1	Top	24
S2-1, S2,2	0.3	0.3	3	2	Top	24
S3-1, S3-2	0.3	0.3	3	3	Top	24
S4-1, S4-2	0.3	0.3	3	4	Top	24
S5-1, S5-2	0.3	0.3	3	5	Top	24

*The first number refers to the number of injections, and second number to the repetition. For example, S1-2 represents the second repetition of sample with one injection.

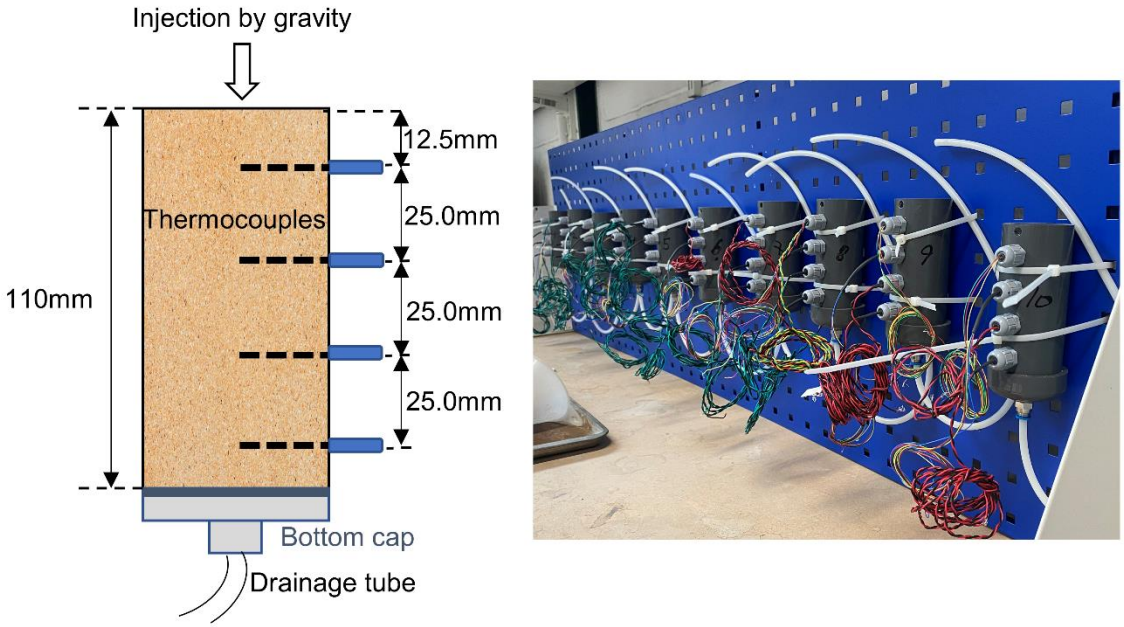

Figure 1. *Schematic set-up of MICP-treated specimens (left). Experimental setup of MICP-treated specimens (right).*

2.2 Experimental measuring device and methods

The thermal conductivity of untreated Hostun sand specimens is 0.24 W/m·K (measured using the commercial thermal property analyser, TEMPOS). This baseline value was compared to the thermal conductivity of the MICP-treated specimens listed in Table 2. For each test, the transient method was applied first. The setup was then left for some time to allow for the soil specimen to reach thermal equilibrium, monitored using the thermocouple temperatures. The steady-state method was subsequently used.

2.2.1 Steady state method

The steady-state method is well-known for its accuracy when measuring soil thermal conductivity (Alrtimi et al., 2014; Xamán et al., 2009). The proposed experimental setup is based on the GHP method. A heating rod embedded within an aluminium disk is placed at the bottom of the specimen to generate a thermal gradient parallel to the axes of the specimen, as shown in Figure 2 (left). An aluminium sink disk placed at the top of the specimen (unheated end) is used to dissipate heat from the outer sides of the specimen. To monitor the temperature gradient of each specimen, four thermocouples were laterally introduced at the desired positions, namely at 12.5 mm ($T_{12.5mm}$), 37.5 mm ($T_{37.5mm}$), 62.5 mm ($T_{62.5mm}$) and 87.5 mm ($T_{87.5mm}$) from the bottom of the specimen in Figure 2a. To minimise radial heat losses and heat losses from the heat source, an insulation layer with low thermal conductivity (polyurethane foam) is used, as shown in Figure 2b. Another two thermocouples were used to monitor the temperature of the heater (T_0) and that of the room. The thermal conductivity test setup is placed within a constant temperature incubator allowing for the room temperature to be adjusted to the desired level. For each test, soil specimens are allowed to reach thermal equilibrium before a constant power (Q) is supplied to

the heater. It should be noted that specimens were treated from top to bottom and inverted for thermal conductivity measurement. Figure 3 (left) shows an example of data collected from the steady state method.

The effective thermal conductivity, λ, can then be calculated using the temperature difference between two thermocouples assuming one dimensional heat flow at steady-state:

$$\lambda = \frac{Q}{A} * \frac{\Delta L}{\Delta T} \quad (1)$$

where Q is the power supplied to the heater, ΔL is the distance between thermocouples, A is the cross-sectional area, and ΔT is the temperature drop across thermocouples.

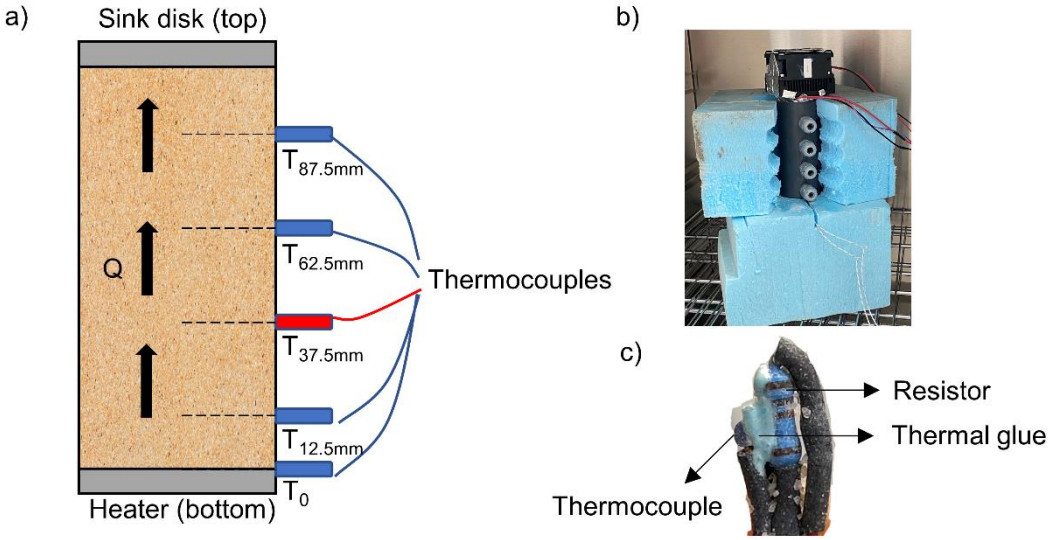

Figure 2. Schematic configuration of the measuring system (red thermocouple is the transient sensor where the thermocouple was attached to a 100-Ohm resistor (a); Experimental setup of the measuring system (b); Transient sensor setup (c).

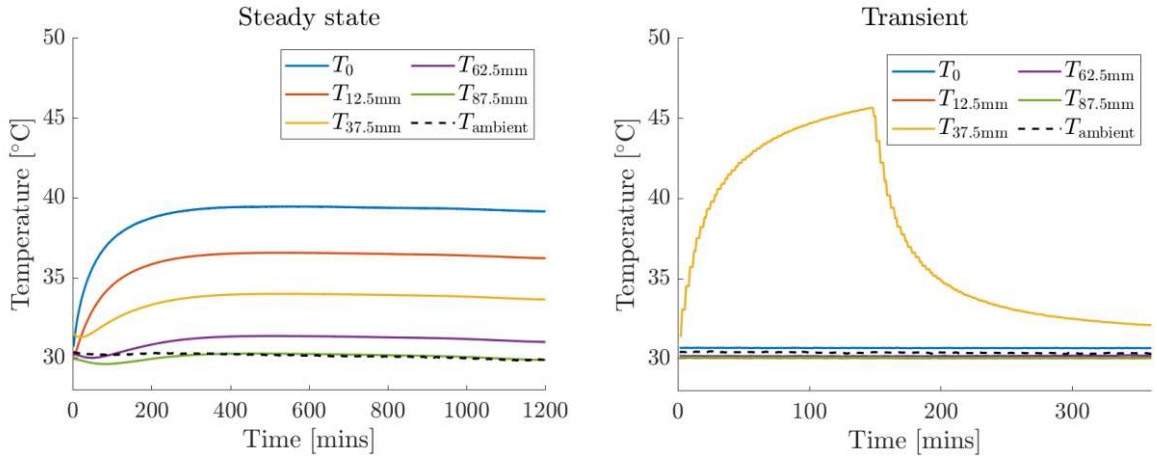

Figure 3. *Example of temperature versus time curve measured with steady-state method along the specimen length (left); example of temperature versus time curve measured from the transient sensor (right)*

2.2.2 Transient method

The newly designed transient thermal sensor consists of a 100-Ohm resistor (height and radius of 6.33 mm and 2.3 mm, respectively) that is used as a heat source, and a thermocouple attached to the resistor for measuring the rate of temperature rise. The sensor is laterally introduced at $T_{37.5mm}$, as shown in red in Figure 2a. A constant power Q is supplied to the resistor during the test, which lasts for 120s, heating up the surrounding soil. An example of the rising temperature over time obtained from the transient

sensor is shown in Figure 3 (right). The power is subsequently switched off for 240s to allow the soil specimen to reach thermal equilibrium. During the steady-state tests, the resistor is disconnected from the power supply, and hence only the thermocouple is used for measuring the temperature of the soil.

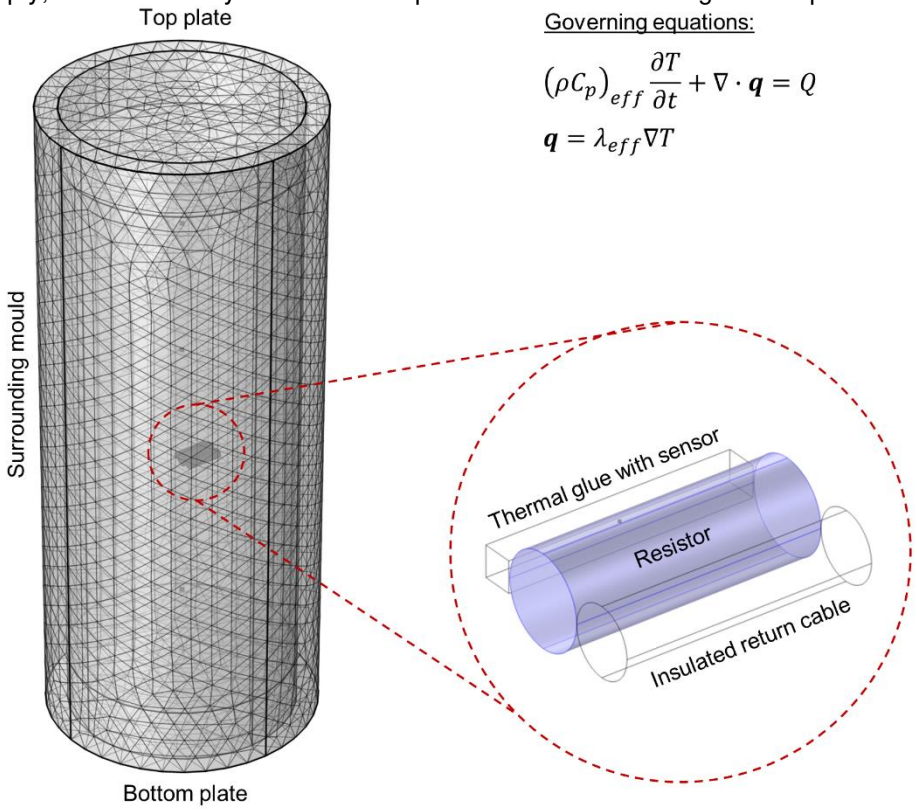

Figure 4. Schematic of the numerical model for the transient sensor method and the model governing equations where T is temperature [°C] and Q the heat source [W/m^3].

For determining the thermal conductivity of MICP-treated sand using the transient method, a detailed three-dimensional (3D) numerical model is created using the finite element package COMSOL Multiphysics®. The model implements the governing equations for conductive heat transfer and simulates the rejection of heat from the resistor to the porous soil and solid elements of the experiment. The MICP-treated soils were modelled on a macro-scale, which assumed homogeneous and continuous soil properties. Given the size and operation time of the transient sensor, the impacted thermal range on the surrounding soil is localised. Therefore, assuming the uniform distribution of MICP precipitation is sufficient in the model. Thermal insulation is applied on the side boundaries and a fixed temperature equal to the measured pre-experiment soil temperature is applied on to top and bottom boundaries, which are too far from the resistor to be affected thermally, and Q is used as input. Table 3 presents the values for the thermal properties used in the modelling and a schematic of the numerical model is shown in Figure 4. A forward simulation technique is employed to estimate thermal conductivity (Santamarina et al., 2005), where the thermal conductivity value of the soil is varied and resulting temperature increases are compared against the experimentally obtained data. The value of thermal conductivity corresponds to the comparison with the lowest mean squared error over the duration of the test.

Table 3. *Key inputs of the numerical model*

Material	**Thermal conductivity, λ** $[W/(m \cdot K)]$	**Specific Heat Capacity, C_p** $[J/(kg \cdot K)]$	**Density, ρ** $[kg/m^3]$	**Porosity, n** [-]
Soil	varies	800	2650	0.4
Surrounding mould	0.1	900	1760	-
Thermal glue	1.1	2092	1850	-
Resistor	600	500	2000	-
Insulated cable	0.03	1300	20	-

3 RESULTS AND DISCUSSION

3.1 MICP-treated sand thermal conductivity

A comparison of the thermal conductivity values found using the steady-state method, between untreated (highlighted in red) and MICP-treated sand is presented in Figure 5, where the averaged $CaCO_3$ content of the vertical profile is used as the representative $CaCO_3$ content for a given specimen. The results show a clear increase in thermal conductivity due to the MICP treatment, where a $CaCO_3$ of 1% results in a 200% increase in the sand thermal conductivity, which is in agreement with the experimental results from Venuleo et al. (2016). This increase is significant and can substantially improve the coefficient of performance of energy geo-structures embedded within treated soil. Furthermore, the results shown indicate that, the greater the $CaCO_3$ content, the higher thermal conductivity values can be achieved. Though there are a few outliers, likely due to heterogeneity in $CaCO_3$ precipitation within the specimens, the positive correlation between calcium carbonate content and thermal conductivity is apparent with a correlation value of 0.71.

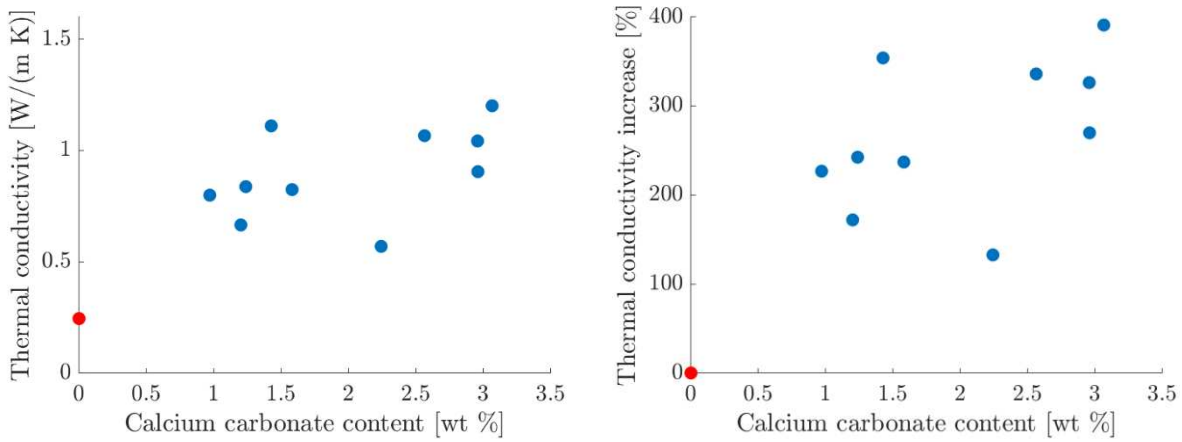

Figure 5. *Steady-state method results: thermal conductivity versus $CaCO_3$ content of the MICP-treated specimens (left). Improvement in thermal conductivity due to MICP treatment (right). Thermal conductivity of untreated sand is highlighted in red.*

3.2 Transient sensor validation

The thermal conductivity values obtained from the comparison of the transient temperature profiles against numerically generated ones are given in Figure 6 (left) for the different levels of calcium carbonate content. The results follow the same trend with those obtained using the steady-state approach, showing a clear positive correlation between calcium carbonate content and thermal conductivity. However, the values obtained via the transient sensor are lower, in the range of about 30% lower. The main reason for such discrepancies, apart from instrumentation errors, could be the heterogeneity. While the numerical model assumes homogeneous thermal properties in the soil, the formation of $CaCO_3$ could lead to heterogeneity in the thermal conductivity distribution. In addition, although part of the insulated returned cable was considered in the model (Figure 4), parallel to the sensor, its exact placement as well as the insulation at the ends of the resistor could provide additional discrepancies. Further work is being undertaken to explore and reduce these discrepancies, as well as develop accessible means to interpret the sensor results. Currently, the accuracy of the thermal conductivity calculated using the transient sensor is of about 70%.

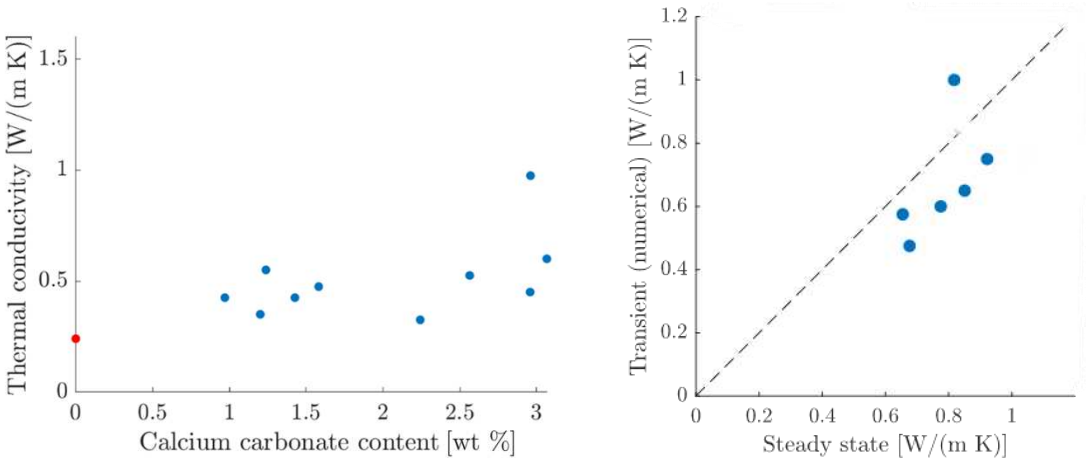

Figure 6. *Transient sensor results: thermal conductivity versus $CaCO_3$ content of the MICP-treated specimens (left). Comparison of transient against steady state results (right).*

4 CONCLUSIONS

This work explores the increase in thermal conductivity of dry sand due to treatment with MICP. Experimental results indicate that the $CaCO_3$ content has a positive correlation with the sand thermal conductivity. The reason for this property enhancement is the formation of $CaCO_3$ crystals, which can serve as thermal bridges that connect soil particles previously separated by air gaps. Since the thermal conductivity of $CaCO_3$ is greater than that of air, the effective thermal conductivity of soil is improved by the presence of these bridges. An increase in conductivity of about 200% is observed for a $CaCO_3$ content of 1 %, which is in agreement with results from the limited available literature. Hence, MICP-treated sand shows potential to contribute towards the wider application of energy geo-structures, particularly geothermal pavements since the road base generally has more voids and is in dry/unsaturated conditions.

Furthermore, this paper introduces a new transient sensor method for measuring soil thermal conductivity. This sensor is low in cost, non-destructive and relatively small, and thus can be easily implemented in laboratory scale tests and field measurements. In this work, the sensor is used to quantify MICP-treated sand thermal conductivity and the results are compared with values obtained using the GHP steady-state method. While both methods show the same trend in the results, with the thermal conductivity increasing with increasing $CaCO_3$ content, the transient sensor results underestimate this increase, with an accuracy of about 70%. The results suggest that the sensor has potential to contribute to quantifying soil thermal properties, specifically for MICP treated conditions, and further research on the application of the transient sensor is underway.

5 ACKNOWLEDGEMENTS

Funding from the Australian Research Council (ARC) (project numbers LP200100052) and the University of Melbourne is much appreciated. The authors would like to thank John Chandler, Kristian Pether, Mark Smith and Chris McGinnie for facilitating the experiments. The second author would also like to acknowledge the Research Fellowship provided by King's College at the University of Cambridge.

REFERENCES

Akrouch, G. A., Sánchez, M., & Briaud, J.-L. (2015). Effect of the Unsaturated Soil Condition on the Thermal Efficiency of Energy Piles. In *IFCEE 2015* (pp. 1618-1627).

Alrtimi, A., Rouainia, M., & Haigh, S. (2016). Thermal conductivity of a sandy soil. *Applied Thermal Engineering, 106*, 551-560. doi:10.1016/j.applthermaleng.2016.06.012

Alrtimi, A., Rouainia, M., & Manning, D. A. C. (2014). An improved steady-state apparatus for measuring thermal conductivity of soils. *International Journal of Heat and Mass Transfer, 72*, 630-636. doi:10.1016/j.ijheatmasstransfer.2014.01.034

Arulrajah, A., Ghorbani, B., Narsilio, G., Horpibulsuk, S., & Leong, M. (2021). Thermal performance of geothermal pavements constructed with demolition wastes. *Geomechanics for Energy and the Environment*. doi:10.1016/j.gete.2021.100253

Barla, M., Di Donna, A., & Santi, A. (2020). Energy and mechanical aspects on the thermal activation of diaphragm walls for heating and cooling. *Renewable Energy, 147*, 2654-2663. doi:10.1016/j.renene.2018.10.074

Bidarmaghz, A., & Narsilio, G. A. (2018). Heat exchange mechanisms in energy tunnel systems. *Geomechanics for Energy and the Environment, 16*, 83-95. doi:10.1016/j.gete.2018.07.004

Bourne-Webb, P., Burlon, S., Javed, S., Kürten, S., & Loveridge, F. (2016). Analysis and design methods for energy geostructures. *Renewable and Sustainable Energy Reviews, 65*, 402-419. doi:10.1016/j.rser.2016.06.046

Brandl, H. (2006). Energy foundations and other thermo-active ground structures. *Géotechnique, 56*(2), 81-122. doi:10.1680/geot.2006.56.2.81

Chen, S. X. (2008). Thermal conductivity of sands. *Heat and Mass Transfer, 44*(10), 1241-1246. doi:10.1007/s00231-007-0357-1

Clarà Saracho, A., Haigh, S. K., & Ehsan Jorat, M. (2021). Flume study on the effects of microbial induced calcium carbonate precipitation (MICP) on the erosional behaviour of fine sand. *Géotechnique, 71*(12), 1135-1149. doi:10.1680/jgeot.19.P.350

DeJong, J. T., Mortensen, B. M., Martinez, B. C., & Nelson, D. C. (2010). Bio-mediated soil improvement. *Ecological Engineering, 36*(2), 197-210.

del-Castillo-García, G., Borinaga-Treviño, R., Sañudo-Fontaneda, L. A., & Pascual-Muñoz, P. (2013). Influence of pervious pavement systems on heat dissipation from a horizontal geothermal system. *European Journal of Environmental and Civil Engineering, 17*(10), 956-967. doi:10.1080/19648189.2013.837842

Di Sipio, E., & Bertermann, D. (2017). Factors Influencing the Thermal Efficiency of Horizontal Ground Heat Exchangers. *Energies, 10*(11). doi:10.3390/en10111897

Eugster, W. J. (2007). Road and Bridge Heating Using Geothermal Energy. Overview and Examples. *Proceedings European Geothermal Congress*.

Gu, X., Makasis, N., Motamedi, Y., Narsilio, G. A., Arulrajah, A., & Horpibulsuk, S. (2021). Geothermal pavements: field observations, numerical modelling and long-term performance. *Géotechnique*, 1-48. doi:10.1680/jgeot.20.P.296

Haigh, S. K. (2012). Thermal conductivity of sands. *Géotechnique, 62*(7), 617-625. doi:10.1680/geot.11.P.043

Insana, A., & Barla, M. (2020). Experimental and numerical investigations on the energy performance of a thermo-active tunnel. *Renewable Energy, 152*, 781-792. doi:10.1016/j.renene.2020.01.086

Kavanaugh, S. P. (2000). *Field tests for ground thermal properties--methods and impact on ground-source heat pump design*. Retrieved from

Kersten, M. S. (1949). Laboratory research for the determination of thermal properties of soils.

Makasis, N., Narsilio, G. A., Bidarmaghz, A., Johnston, I. W., & Zhong, Y. (2020). The importance of boundary conditions on the modelling of energy retaining walls. *Computers and Geotechnics, 120*. doi:10.1016/j.compgeo.2019.103399

Martinez, A., Huang, L., & Gomez, M. G. (2019). Thermal conductivity of MICP-treated sands at varying degrees of saturation. *Géotechnique Letters, 9*(1), 15-21. doi:10.1680/jgele.18.00126

Mujah, D., Shahin, M. A., & Cheng, L. (2016). State-of-the-Art Review of Biocementation by Microbially Induced Calcite Precipitation (MICP) for Soil Stabilization. *Geomicrobiology Journal, 34*(6), 524-537. doi:10.1080/01490451.2016.1225866

Narsilio, G. A., Kress, J., & Yun, T. S. (2010). Characterisation of conduction phenomena in soils at the particle-scale: Finite element analyses in conjunction with synthetic 3D imaging. *Computers and Geotechnics, 37*(7-8), 828-836. doi:10.1016/j.compgeo.2010.07.002

Nusier, O., & Abu-Hamdeh, N. (2003). Laboratory techniques to evaluate thermal conductivity for some soils. *Heat and Mass Transfer, 39*(2), 119-123. doi:10.1007/s00231-002-0295-x

Porter, H., Dhami, N. K., & Mukherjee, A. (2018). Sustainable road bases with microbial precipitation. *Proceedings of the Institution of Civil Engineers - Construction Materials, 171*(3), 95-108. doi:10.1680/jcoma.16.00075

Rahman, M. M., Hora, R. N., Ahenkorah, I., Beecham, S., Karim, M. R., & Iqbal, A. (2020). State-of-the-Art Review of Microbial-Induced Calcite Precipitation and Its Sustainability in Engineering Applications. *Sustainability, 12*(15), 6281. Retrieved from https://www.mdpi.com/2071-1050/12/15/6281

Rizvi, Z. H., Nikolić, M., & Wuttke, F. (2019). Lattice element method for simulations of failure in bio-cemented sands. *Granular Matter, 21*(2). doi:10.1007/s10035-019-0878-6

Santamarina, J. C., & Fratta, D. (2005). *Discrete signals and inverse problems: An Introduction for Engineers and Scientists*. UK: John Wiley & Sons.

Seong, J., Haigh, S. K., Madabhushi, S. P. G., Shrivastava, R., Veluvolu, R., & Padhy, P. (2022). On seismic protection of wind turbine foundations founded on liquefiable soils. *Soil Dynamics and Earthquake Engineering, 159*. doi:10.1016/j.soildyn.2022.107327

Venuleo, S., Laloui, L., Terzis, D., Hueckel, T., & Hassan, M. (2016). Microbially induced calcite precipitation effect on soil thermal conductivity. *Géotechnique Letters, 6*(1), 39-44. doi:10.1680/jgele.15.00125

Xamán, J., Lira, L., & Arce, J. (2009). Analysis of the temperature distribution in a guarded hot plate apparatus for measuring thermal conductivity. *Applied Thermal Engineering, 29*(4), 617-623. doi:10.1016/j.applthermaleng.2008.03.033

Xiao, P., Liu, H., Xiao, Y., Stuedlein, A. W., & Evans, T. M. (2018). Liquefaction resistance of bio-cemented calcareous sand. *Soil Dynamics and Earthquake Engineering, 107*, 9-19. doi:10.1016/j.soildyn.2018.01.008

Xiao, Y., Tang, Y., Ma, G., McCartney, J. S., & Chu, J. (2021). Thermal Conductivity of Biocemented Graded Sands. *Journal of Geotechnical and Geoenvironmental Engineering, 147*(10). doi:10.1061/(asce)gt.1943-5606.0002621

Xiao, Y., Xiao, W., Ma, G., He, X., Wu, H., & Shi, J. (2022). Mechanical Performance of Biotreated Sandy Road Bases. *Journal of Performance of Constructed Facilities, 36*(1). doi:10.1061/(asce)cf.1943-5509.0001671

Yun, T. S., & Santamarina, J. C. (2007). Fundamental study of thermal conduction in dry soils. *Granular Matter, 10*(3), 197-207. doi:10.1007/s10035-007-0051-5